

Vortical Structures of an Impinging Jet in Cross-flow

Keith J. Kucinskas¹

¹University of Hartford

6 Pioneer Drive, West Hartford, CT 06117. Keith.kucinskas@gmail.com

Abstract: The analysis of an impinging jet in a cross-flow and the resulting vortical structures are presented. A computational fluid dynamics simulation utilizing the k- ϵ model for turbulence is validated by comparing the results to previous experimental and theoretical studies conducted in air. The model was then altered utilizing the hydraulic analogy for an experiment planned within a water tunnel that will maximize the visualization capabilities of the secondary flows that develop. Solutions to this hydraulic version of the computational fluid dynamic model were completed in both steady and time dependent states. The features of the flow structures and insight into the physics that form them are established.

Keywords: horseshoe vortex, impinging jet, secondary flow, hydraulic analogy

1. Introduction

Aircraft engines have evolved to become complex machines that enable people and goods to travel vast distances over a relatively short period of time. In traditional avionics, gas turbines have become the dominant form of engine architecture in both military and commercial applications. In particular, the turbofan construction has become prevalent in most aircrafts that are airborne today. These commercial turbofans are comprised of an inlet diffuser, a fan, a compressor, a combustor (burner), a turbine, and nozzles as the major modules.

Flow through this machine can be quite complex. The main flow moves from forward to aft in the axial direction, but there are also circumferential flows imparted by the turning airfoils. Furthermore, there are secondary flows induced throughout the compressor, combustor, and turbine modules that result in different physical behaviors of the various components. These secondary flows typically debit the efficiency of the modules. Furthermore these vortical structures also affect the thermodynamic heat transfer mechanisms essential for the cooling of high temperature turbine airfoils.

This study examines vortical structures of an impinging jet on a cube in a cross-flow using commercial software package COMSOL. First, a computational fluid dynamic model is developed and validated using previous experimental studies. The model is then reconfigured to simulate the same dynamics with water as the flow media. Using water allows for easier flow observations than that of the air experiments. Future experimentation is planned at the University of Hartford in a water tunnel laboratory. The results and conclusions from the computational fluid dynamics study presented here could then be compared to actual observed flows in the water tunnel. Due to the similarities of the vortical structures developed within the impinging jet in cross-flow model with that of the various vortices studied in turbomachinery, the lessons learned are transferrable to the complex geometry of airfoils.

2. Impinging Jet in Cross-flow Validation Modeling

The impinging jet within a cross-flow has been studied in several publications [4]. The investigation presented here utilizes the results in these publications in order to validate the model intended for use in the water tunnel. The actual experimental data was gathered utilizing air as the flow media for a wall mounted cube in cross-flow and the results were captured using particle image velocimetry (PIV) [5]. In another study the flow characteristics were predicted using a Reynolds Stress Model (RSM) and a $\overline{v^2} - f$ model [4]. The Reynolds stress model (RSM) of turbulence is perhaps the most complex model used by engineers to estimate the influence of turbulence on the mean flow. The motivation of its development comes from the inability of the k- ϵ model to cope with major anisotropy in the turbulence history effects [1]. The $\overline{v^2} - f$ model of turbulence is similar to the k- ϵ model except it includes some near-wall turbulence anisotropy and non-local pressure strain effects [4]. The computational models resulted in data that simulated the vortical structures found using the PIV, but slightly differed on magnitudes of

velocity and kinetic energy. The study presented here instead uses the commercially available COMSOL package that utilizes the k- ϵ model to predict the turbulent behavior. The results of the COMSOL study are compared to that of the PIV data, $\overline{v^2} - f$ model and Reynolds Stress Model in order to validate the methods used prior to applying the technique in the water tunnel simulation.

2.1 Experimental Setup

The numerical models are all validated using PIV measurements [5]. The experimental set-up as summarized in Fig. 1 consists of an air passage with five cubes mounted in line in the middle of the tunnel. The length of each cube side is 15 mm. The distance between a pair of cubes is 60 mm. The tunnel has a height H of 30 mm and a width of 360 mm. The impinging jet originates at a circular hole above the center of the third cube with a diameter D of 12 mm [5]. Note that this cube has a heated isothermal core for the purpose of a heat transfer study. This report does not analyze the details of this heat transfer model; however, the COMSOL validation model will take into account this heating effect with respect to flow, as to eliminate it as a source of potential error.

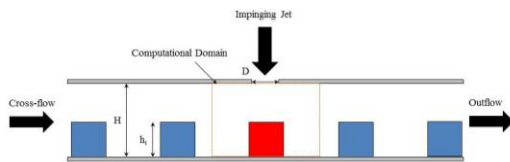


Figure 1. Schematic of Experimental Setup

2.2 Computational Domain

The geometric modeling is based on the previous studies [4]. In this simulation only one cube is modeled. Furthermore the width of the tunnel has been drastically reduced from 360 mm to decrease the computing time. Figure 2 shows the fundamental construct of the geometry that is modeled. Table 1 yields the data that bounds the geometric components.

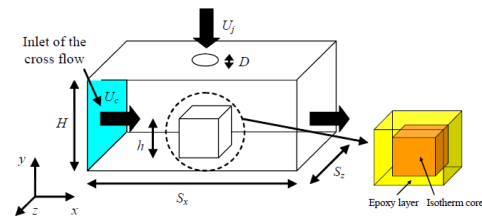


Figure 2. Schematic of Computational Geometry [4]

Variable	Value	Units	Description
D	12	mm	Diameter of hole
h_t	15	mm	Cube side length
H	30	mm	Box height
S_x	60	mm	Box length
S_z	60	mm	Box width
δ_c	1.5	mm	Epoxy thickness
U_c	1.73	m/s	Cross-flow velocity
U_j	10	m/s	Jet flow velocity
U_j/U_c	5.78	N/A	Velocity ratio

Table 1. Physical Geometry Variables and Velocities

The given values were used to create a model in the COMSOL as seen in Fig. 3. The modeled geometry utilized a cylindrical curve to represent an area where the jet boundaries will likely be dominant. No physical boundaries were applied to this cylindrical geometry so the analysis will be unaffected by its presence. It does however yield a surface that can have its mesh manually manipulated. This modeling approach and software package differs from the procedure of the previous studies [4].

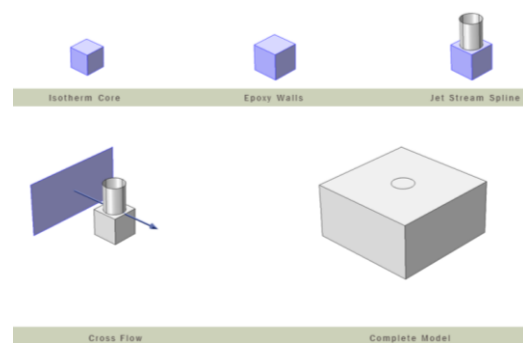


Figure 3. Model Geometry in COMSOL

2.3 Mesh Details

The model's mesh was initially defined as utilizing the default physically-controlled settings available in COMSOL. The boundaries were then manually manipulated to add mesh refinement at the key areas of interest. The impinging surface of the cube was selected and chosen to have an extra fine mesh as per the default mesh sizing available in the software package. The cylindrical curve that enclosed the expected area of the jet was also selected to have this extra fine mesh. The remaining fluid was modeled with the fine mesh settings available. The boundary surfaces of the cube were modeled using the finer mesh settings whereas the mesh of the isothermal core was left coarse. This strategy allowed for the computation to be the most refined at the areas of greatest interest. The size of the cells can be viewed in Fig. 4 which shows a cross-sectional view with the differences in mesh size through a color map. The most mesh refinement is at the expected boundary of the jet and the cube face surfaces.

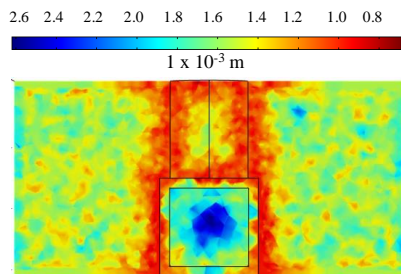


Figure 4. Model Geometry in COMSOL

3. Fundamental Physics

The fundamental equations discussed in this section outline the physics that were used in order to achieve a solution. Note that body forces such as gravity were ignored in order to simplify the COMSOL model.

3.1 Flow Regime

In order to define the flow, the Reynolds number must be calculated. This is a dimensionless ratio between the inertia forces and viscous forces of the fluid governed by Eq. 1.

$$Re = \frac{\rho \cdot U \cdot L_{char}}{\mu} \quad (1)$$

The characteristic length depends on the type of geometry used. Since previous literature [4] did not provide definition of this variable, the characteristic length of the cross-flow was considered to be the hydraulic diameter as defined in Eq. 2.

$$D_{H,c} = \frac{4A}{P} = \frac{2(S_z \cdot H)}{(S_z + H)} = 0.04m \quad (2)$$

This value was then used to compute the Reynolds number for the cross-flow as seen in Eq. 3.

$$Re_c = \frac{\rho_a \cdot U_c \cdot D_{H,c}}{\mu_a} = 4,657.17 \quad (3)$$

The computed value in Eq. 3 is comparable to the value in the previous study of 4,725 [4].

The characteristic length for the impinging jet is the diameter of the jet. The value of the Reynolds number is calculated using Eq. 4.

$$Re_j = \frac{\rho_a \cdot U_j \cdot D}{\mu_a} \quad (4)$$

The computed value in Eq. 4 results in a Reynolds number of 8,076.2 when a jet velocity of 10 m/s is utilized. This is comparable to the previous documentation that recorded this value as 8,217 [4]. Based on the computation of these Reynolds numbers, the flow regime is considered turbulent.

3.2 Turbulence Model

A fundamental set of equations often used to describe fluid flow are the Navier Stokes equations. These equations are derived by applying Newton's second law regarding momentum to fluid motion. In order to solve such a complex set of equations the Reynolds decomposition is applied where an instantaneous quantity is decomposed into its time-averaged fluctuating quantities. This method is known as Reynolds Averaged Navier Stokes (RANS). There are however more unknowns than equations when studying a turbulent flow. This is known as the closure problem that will be solved in this study by the k-ε model.

The k-ε model is a common turbulence model. This model includes two extra transport variables to represent properties in the flow. One of these added transport parameters is k, the turbulent kinetic energy. The other is ε, the

turbulent dissipation that determines the scale of the turbulence. This model is defined by Eq. 5 – 8.

$$\rho(u_i \cdot \nabla)k = \nabla \cdot \left[\left(\mu + \frac{\mu_t}{\sigma_k} \right) \nabla k \right] + P_k - \rho \varepsilon \quad (5)$$

$$\rho(u_i \cdot \nabla)\varepsilon = \nabla \cdot \left[\left(\mu + \frac{\mu_t}{\sigma_\varepsilon} \right) \nabla \varepsilon \right] + C_{\varepsilon 1} \frac{\varepsilon}{k} P_k - C_{\varepsilon 2} \rho \frac{\varepsilon^2}{k} \quad (6)$$

$$\mu_t = \rho C_\mu \frac{k^2}{\varepsilon} \quad (7)$$

$$P_k = \mu_t \left[\nabla u_i : (\nabla u_i + (\nabla u_i)^T) - \frac{2}{3} (\nabla u_i)^2 \right] - \frac{2}{3} \rho k \nabla \cdot u_i \quad (8)$$

Constant values are assumed for many of the coefficients:

$$C_{\varepsilon 1} = 1.44$$

$$C_{\varepsilon 2} = 1.92$$

$$C_\mu = 0.09$$

$$\sigma_k = 1.0$$

$$\sigma_\varepsilon = 1.3$$

At the walls, a no slip condition is assumed. In order to evaluate flow properly in these regions Eq. 9 is required.

$$\varepsilon = \rho \frac{C_\mu k^2}{\kappa_V \delta_w \mu} \quad (9)$$

4. Validation Model Comparison

The most critical comparison made between previous literature and the validation study focuses on the data gathered with respect to the velocity magnitude throughout the flow [4]. Figure 5 shows the velocity magnitude from the previous studies using RSM and $\overline{v^2} - f$ turbulence models, the PIV measurements, and this validation study in a cross-section through the center of the cube at the plane of symmetry.

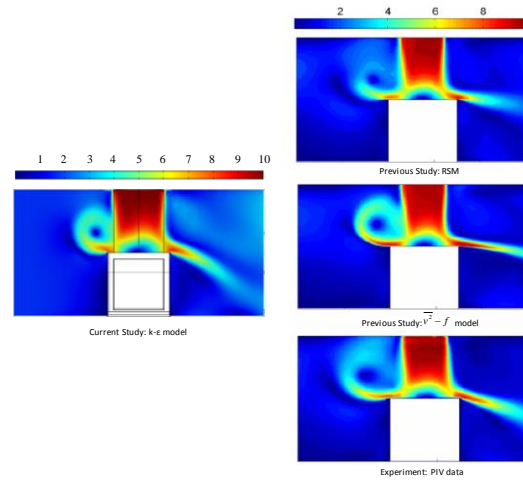


Figure 5. Contours of Velocity Magnitude (Left Hand Side: Current Study, Right Hand Side: Previous Studies) [4]

The left hand side plot in Fig. 5 depicts the current study utilizing the k-ε model with a jet velocity of 10 m/s. The right hand side plots are that of the previous studies [4]. In each of these analysis, a vortex can be plainly seen where the cross-flow meets the impinging jet. The current study shows a vortex formed of comparable size to that of the previous studies that is approximately 80% of the cube height. These results of the current study are very similar to that of the $\overline{v^2} - f$ model. As compared to the PIV data however reveals that the k-ε model overestimates the velocity magnitude at the top of the vortex. Furthermore, the trailing edge of the cube depicts a curved shape in the velocity profile in the current simulation that was not recorded with the PIV. Despite this it is still more accurate than the RSM of the previous studies and considered suitable as a valid model for the hydraulic version of the experiment.

5. Impinging Jet in Cross-flow within a Water Tunnel

With the water tunnel donated to the University of Hartford from United Technologies Research Center, the impinging jet in cross-flow experiment is a prime candidate for studying vortical structures. This section will explain the benefits of secondary flow visualization by using water as the flow media. A new model set-up is made with a computational domain that reflects the same flow

as in the air model. The flows within the water tunnel version of the experiment are predicted and analyzed utilizing the k- ϵ model in both a steady state and time dependent conditions.

Flow visualizations of secondary flows are not simple within a gas flow environment. The equipment to pressurize the air, attain a uniform velocity profile, and visualize the flow are expensive. Even the models of the aerodynamic bodies tend to become quite expensive as they must endure the high loads due to the drag and lift forces at high wind velocities [2]. Furthermore, the engineering time necessary to adequately observe the subtleties of complex flow fields can be quite lengthy.

The other challenge in studying the flow of air in a wind tunnel is accuracy due to a scaling factor. Many experiments attempt to test high velocity flow of an open channel flow over aerodynamic body within a test cell. This test cell adds a variable where the air can easily be inadvertently choked between the aerodynamic body and the test cell walls due to a nozzle effect. A couple of the ways to avoid such a condition is by making a larger test cell which would require a higher mass flow rate and therefore be more expensive, or scale the model down significantly which could make vortex studies difficult.

In order to offset the expense and challenges of wind tunnel studies the hydraulic analogy is often utilized in the study of aerodynamic bodies. Essentially the same flow of air can be mimicked with a fluid at much slower velocities. The hydraulic analogy is useful for simulating high-speed ideal gas flow with shallow water because it becomes much more convenient and accurate to study due to the speed being orders of magnitude slower than that of the gas flow [2]. Since 1983, NASA has been taking advantage of this analogy through their Flow Visualization Facility (FVF) at Edwards Air Force Base, California. Since the start of its operation, the FVF's primary use has been to study three-dimensional vortex flow on aircraft configurations. Because of the low Reynolds numbers obtainable in a water tunnel, NASA has found it is best used to investigate flow regimes where the vortex flow is dominant over viscous flow effects [3]. The impinging jet in a cross-flow creates the same flow regime, and is therefore a suitable candidate for flow visualization via the use of a water table.

The hydraulic analogy is made possible by keeping the dimensionless Reynolds number and jet to cross flow velocity ratio constant within the flow fields between the air experiment and the water tunnel research in this investigation. Keeping all other variables constant at room temperature and sea level pressure, the water velocity required to create the same flow is over fourteen times slower than that of the air flow. This is due to the large change in density between the different flow media. Despite this massive change in velocity, the vortex structures will theoretically be very similar due to utilizing the constant Reynolds number. A view of the test cell within the water tunnel is depicted in Fig. 6.

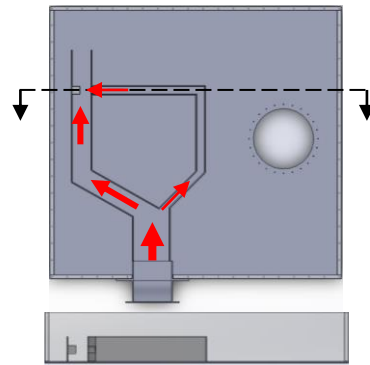


Figure 6. Top and Section View of Test Cell

In this portion of the study, English units are utilized. Furthermore a larger cube is modeled that is 2 inches tall versus the airflow experiment's 0.591 inch (15 mm) cube to further increase the capability of flow visualizations. This results in a water jet flow of 0.641 ft/s that is over 50 times slower than the air study. The cross-flow has a corresponding average velocity of 0.111 ft/s.

6. Steady State Water Model Results

This section focuses on the steady state results of the water experiment. Streamline plots are generated through the use of the model. Then the flow is examined through the use of multiple cross-sections.

6.1 Streamline Analysis

The vortical structures of the steady state water model that were created through this investigation are represented in the streamline plots of Fig. 7. The horseshoe vortex is represented by the blue streamlines. This vortex forms at the front face of the cube at a saddle point where the separated jet flow collides with the cross-flow. This results in two counter-rotating vortex pairs that diverge from the center of the cube. These counter rotating vortices have an increasing diameter as they flow to the rear side of the computational domain. At the rear side of the cube, up-wash vortices are formed and are depicted with green streamlines in Fig. 7. This up-wash vortical structure forms at this point due to the cross-flow wrapping around the cube and forming a wake at the rear side. Figure 7 graphs (D) and (C) illustrate two down-wash vortices with orange streamlines. These vortices are formed due to the cross-flow meeting the jet flow above the area of the horseshoe vortex. They are formed in a similar fashion as a wake does behind a cube; however they are the developed behind a relatively high velocity jet and not a solid body.

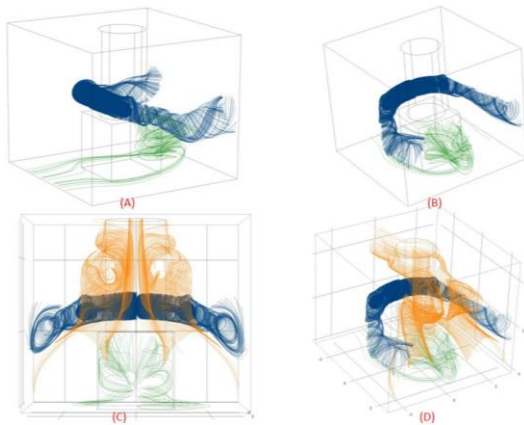


Figure 7. Streamline Plots of the Steady State Water Model at Various Angles

6.2 Cross-Sectional Analysis

The steady state flow of the water model that was simulated in this study was further analyzed by creating multiple cut planes parallel to the XY plane. These cut planes were made at $z = -2.3$, -1.725 , -1.15 , -0.8625 , -0.575 , -0.2875 , and 0 inches. Figure 8 shows the first cut plane and

the direction of the progressive cuts. Note that at $z = 0$ inches, the cut plane bisects the cube along the XY plane.

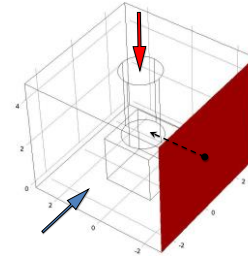


Figure 8. XY Cut Plane Progression

Figure 9 shows the velocity contour plots generated at the multiple cut planes described above. Then Fig. 10 illustrates the same cut planes with plots that yield the magnitude of the velocity at these different points.

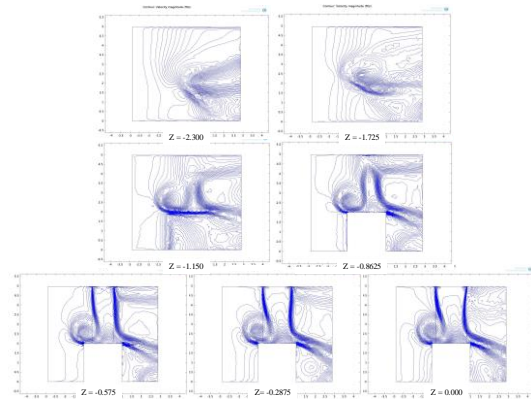


Figure 9. Velocity Contour Plots at Cut Planes Parallel to the XY Plane

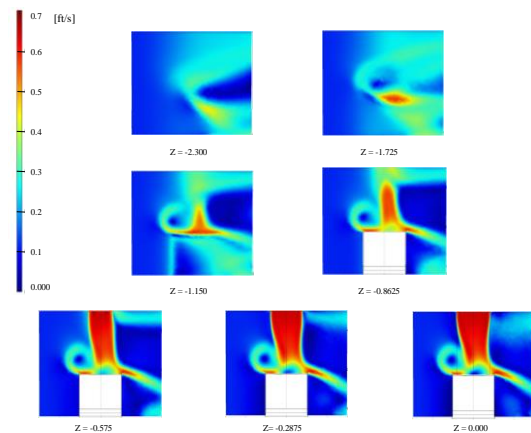


Figure 10. Velocity Magnitude Contour Plots at Cut Planes Parallel to the XY Plane

7. Transient Water Model Results

In this section, the time dependent model of the impinging jet in cross-flow with water as the flow medium is analyzed. A cross-section that bisects the cube along the XY plane was evaluated at multiple time steps in an effort to understand how the flow developed. The dynamics that form the multiple vortices are better understood by analyzing these plots of the velocity contours and velocity magnitude. They are depicted in Fig. 11 – 12 at time 0.5, 0.7, 0.9, 1.0, 1.1, 1.3, 1.5, 2.0, 2.5, 4.0, 6.0, and 10 seconds.

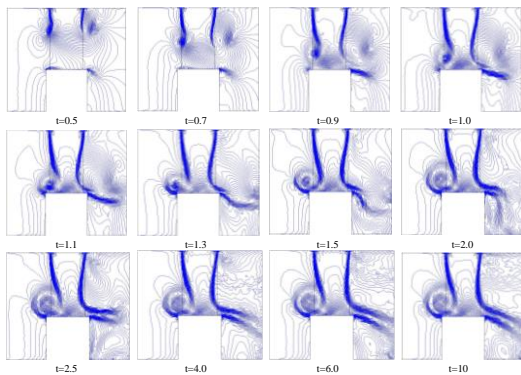


Figure 11. Time Dependent Velocity Contour Plots at the XY Cross-Sectional Plane

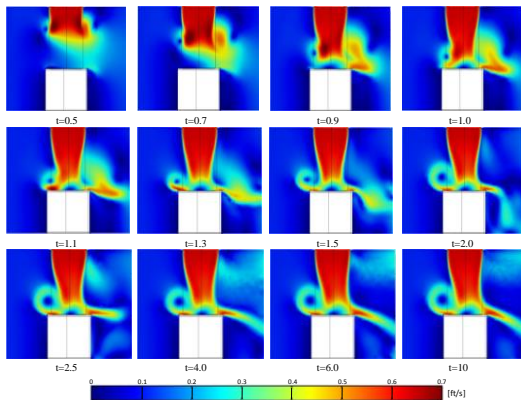


Figure 12. Time Dependent Velocity Magnitude Plots at the XY Cross-Sectional Plane

Figures 11-12 clearly indicate the development of the horseshoe vortex occurs quickly. The high velocity point at the aft end of the cube forms less rapidly and reaches steady state at approximately 10 seconds.

8. Conclusions

The water media impinging jet in a cross-flow can be qualitatively modeled utilizing the COMSOL k- ϵ model and the hydraulic analogy. By keeping the Reynolds numbers and velocity ratios constant, a low speed flow of the complex secondary flows can be made that would be less expensive to visualize in a lab environment than a study using air. Results indicate the presence of a horseshoe vortex, counter-rotating vortical pairs, an up-wash vortex, and two down-wash vortices should be expected.

By utilizing the results found in this examination, a future study in a water tunnel can be completed where the predicted can be compared with actual experimental data. Confirming the existence, size, and shape of the vortex structures will further validate this study. This physical experiment will be made possible by the refurbishment and construction of a water table donated to the University of Hartford.

8. References

1. Davidson, P. A. 2004. *Turbulence: An Introduction for Scientists and Engineers*. Oxford: Oxford UP
2. Kumar, V., I. Ng., G.J. Sheard, K. Hourigan, A. Fouras. 2009. "Hydraulic Analogy Examination of Underexpanded Jet Shock Cells using Reference Image Topography." 8th International Symposium on Particle Image Velocimetry – PIV09, August 25-28 in Melbourne Australia
3. NASA. Flow Visualization Facility. http://www.nasa.gov/centers/dryden/history/past_projects/FVF/index_prt.htm (accessed July 15, 2013)
4. Rundstrom, D., B. Moshfegh, and A. Ooi. 2007. "RSM and V2-f Predictions of an Impinging Jet in a Cross Flow on a Heated Surface and on a Pedestal." 16th Australasian Fluid Mechanics Conference: 316-323.
5. Tummers, M. J., M. A. Flikweert, K. Hanjalic, R. Rodink, and B. Moshfesh. 2005. "Impinging Jet Cooling of Wall-mounted Cubes." Proceedings of ERCOFTAC International Symposium on Engineering Turbulence Modeling and Measurements - ETMM6: 773-782